Microsystem Technologies (2023) 29:337–345
https://doi.org/10.1007/s00542-023-05429-6

TECHNICAL PAPER

Dual-band SIW cavity backed antenna loaded with CSRR metameterial

R. Samson Daniel[1]

Received: 16 March 2021 / Accepted: 7 February 2023 / Published online: 17 February 2023

Abstract

A dual-band substrate integrated waveguide (SIW) cavity backed antenna loaded with complementary split ring resonator (CSRR) metamaterial is proposed for WiMAX/WLAN band applications. This antenna uses a rectangular cavity and CSRR slots on the ground plane for dual band radiation. The rectangular SIW cavity resonator produces two cavity modes TE_{110} and TE_{120} into free space owing to array of metallic vias. By introducing CSRR, it excites the lower hybrid modes for realizing a low-profile antenna design at 2.5 GHz due to strong coupling effect in the SIW cavity resonator. The mode theory mechanism is utilized for analysis the designed antenna. The geometry of the fabricated antenna is developed on a low cost FR-4 dielectric substrate with dimensions 30 × 30 × 1.6 mm^3 to resonance at 2.5 GHz and 5.4 GHz. The experimental S_{11}(dB) exhibits a fractional bandwidth of 4% (2.45–2.55 GHz) in the lower resonant frequency of 2.5 GHz and 2.4% (5.33–5.46 GHz) in the higher resonance frequency of 5.4 GHz. The designed antenna possesses significant advantages of low-profile, better S_{11}(dB), planar configuration and unidirectional radiation patterns.

1 Introduction

Recently, substrate integrated waveguide (SIW) cavity backed antennas have been developing as an eminent candidate in modern wireless technology due to better isolation (Kumar et al. 2018), unidirectional pattern (Chaturvedi et al. 2019), high gain (Mukherjee and Biswas 2018), combining planar and non- planar configurations (Nigam et al. 2020), circular polarization (Priya et al. 2020), Phase correction (Gong et al. 2017) and reduce the side lobe level (Gong et al. 2016). These characteristics can be realized using metallic waveguide structure. The rows of metallic vias in SIW are formed to create waveguide side walls for preventing spurious radiation. SIW techniques have been utilized in designing MIC components such as filters (Shi et al. 2018), microwave sensor (Yun and Lim 2014), power divider (Gatti and Rossi 2018) and body area network devices (Chaturvedi 2020). Bow-tie slot (Mukherjee and Biswas 2016) and dumbbell shaped slot (Mukherjee and Biswas 2017) are used to attain hybrid modes in the SIW cavity for achieving multiband frequency response.

Metamaterial is a non-natural electrodynamics substances with negative values of permeability (μ) and permittivity (ε). These specified features can be governed ZOR (Zeroth Order Resonance) for reducing the size of the antenna (Samson Daniel 2020). Complementary split ring resonatorbased metamaterial configurations have been revealed for multiband along with the compact size of the antenna (Samson Daniel et al. 2018b). The series and shunt element of complementary split ring resonator influences electric current to construct a lower mode resonance with better return loss characteristics (Samson Daniel et al. 2018c). The EM radiation is controlled by EM absorber, which includes the permeability and permittivity of the material. Due to the high electrical conductivity, the electromagnetic shielding materials block the transmission radiation to prevent the harmful radiation (Zhang et al. 2021). The amalgamation of green electromagnetic interference with "non-crosstalk" multiple perceptions are beneficial to construct next-generation devices, such as medical treatment, remote sensing and aerospace engineering (Cao et al. 2020). EM response mechanism and their properties of low-dimensional material are used to design nano-micro devices in the microwave frequency range (Cao et al. 2019).

In this article, a low-profile substrate integrated waveguide (SIW) antenna loaded with complementary split ring resonator (CSRR) metamaterial is designed for dual-band operations. To realize lower hybrid modes for antenna

✉ R. Samson Daniel
samson.rapheal@gmail.com

[1] Department of ECE, K.Ramakrishnan College of Engineering, Samayapuram, Tiruchirappalli, India

miniaturization, CSRR metamaterial is loaded on the ground plane. The desired operating bands are achieved by tuning series capacitance and shunt inductance parameters of CSRR. An electrical size of the proposed antenna is 0.25 $\lambda_0 \times 0.25\ \lambda_0 \times 0.0133\ \lambda_0$,where λ_0 is the free space wavelength at $f_0 = 2.5$ GHz. Due to band characteristics of CSRR and its negative permittivity attributes, the proposed fashion is useful to ascertain applications for nanoelectronics and telecommunication devices.

2 Antenna description and simulated results

The designed antenna has been fashioned from a dual-band rectangular SIW cavity backed antenna as described in the prototype (A) of Fig. 1. To attain lower hybrid modes from this rectangular SIW cavity resonator, the complementary split ring resonator (CSRR) metamaterial is loaded on the ground plane as described in the prototype (B) of Fig. 1. CSRR is reasonable to generate electric resonance for achieving dual-band at 2.5 GHz and 5.4 GHz due to the CSRR structural configuration. The slit ($\mathbf{S}_1$) and width ($\mathbf{S}_2$) of the CSRR are preserved as a constant value of 1 mm for homogeneity. The schematic representation of the proposed antenna is depicted in Fig. 2 and its parameters have been listed in Table.1.

The proposed antenna is designed by using Ansys HFSS V.14.0 EM tool. The simulated $\mathbf{S}_{11}$(dB) of Prototype (A) and Prototype (B) are depicted in Fig. 3. The SIW cavity

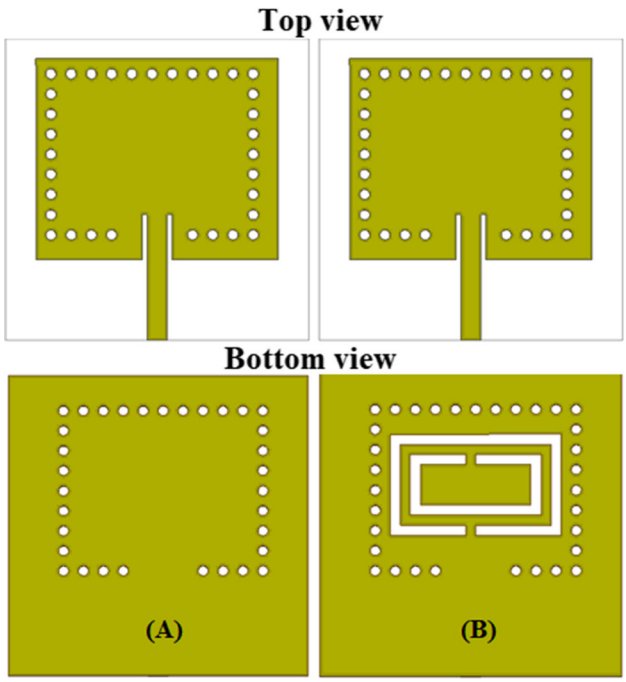

Fig. 1 Prototype geometry

($\mathbf{L_c} \times \mathbf{W_c}$) is realized by using copper claddings with metallic via-array, which constructs the sidewalls of the SIW. The diameter (d) and pitch distance (p) of the metallic vias have been attuned to ensure $\mathbf{d}/\boldsymbol{\lambda}_0 \leq 0.1$ and $d/p \geq 0.5$ for avoiding spurious radiation (Mukherjee and Biswas 2017). The rectangular SIW cavity length ($\mathbf{L_c}$) and width ($\mathbf{W_c}$) are computed from the precise design equation (Chaturvedi 2020).

$$f_r(TE_{mnp'}) = \frac{c}{2\sqrt{\varepsilon_r}}\sqrt{\left(\frac{m}{L}\right)^2+\left(\frac{n}{W}\right)^2+\left(\frac{p'}{h}\right)^2} \quad (1)$$

$$\text{where, } L \text{ or } W = \boldsymbol{L_c} \text{ or } \boldsymbol{W_c} - 1.08\frac{\boldsymbol{d^2}}{\boldsymbol{p}}$$

Here, ε_r is the relative permittivity of the FR-4 dielectric substrate, length of the SIW cavity L_c=17 mm, width of the SIW cavity W_c=21 mm, f_r is the resonance frequency and m, n, p' are mode integers. Thus, it supports TE_{110} mode at 3.53 GHz and TE_{120} mode at 5.83 GHz. CSRR is a resonant behavior as its perimeter is double the resonant wavelength equivalent to cavity mode. Due to CSRR coupling, the fundamental cavity modes (TE_{110} and TE_{120}) become attuned and provides the reconstructed modes TE_{110} and TE_{120} towards the lower resonance frequencies of 2.5 GHz and 5.4 GHz, respectively.

The comparative analysis of the proposed antenna with earlier published work is detailed in Table 2. It has been recognized that the proposed antenna offers dual band operating frequencies with small size equated with previously described works. This paper accentuates CSRR band nature as well as ε-negative for constructing lower hybrid modes.

3 Operating mechanism

The real part input impedance of the rectangular SIW cavity resonator (Prototype A) and rectangular SIW cavity resonator loaded with complementary split ring resonator (CSRR) (Prototype B) are shown in Fig. 4. It is inferred that loading of the CSRR, significantly impacts cavity modes (TE_{110} and TE_{120}) and yields two hybrid modes at 2.5 GHz and 5.4 GHz. Similarly, Fig. 5 explains the same. The electric field distribution of rectangular SIW cavity according to cavity modes TE_{110} (at 3.53 GHz) and TE_{120} (at 5.83 GHz) are illustrated in Fig. 5a, which affects each other after loading the CSRR and produce lower hybrid modes at 2.5 GHz and 5.4 GHz as illustrated in Fig. 5b. Thus, the hybrid modes TE_{110} and TE_{120} are governed predominantly by the CSRR and maximum electric field is induced in the outer aperture of the SIW cavity due to changes in phaseand magnitude of the electric field intensity at the different side of the CSRR slot.

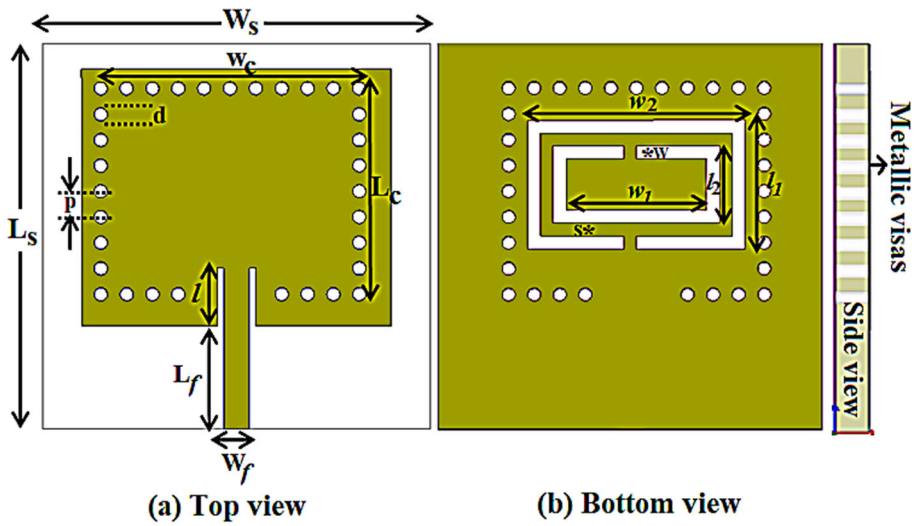

Fig. 2 Schematic representation of the proposed antenna

Table 1 Antenna dimensions

Parameters	Dimensions (mm)
W_s	30
L_s	30
W_c	21
L_c	17
d	1
p	2
W_f	2
l_f	4.5
w	17
l_1	10
w_1	15
l_2	6
w_2	11
s	1
w	1

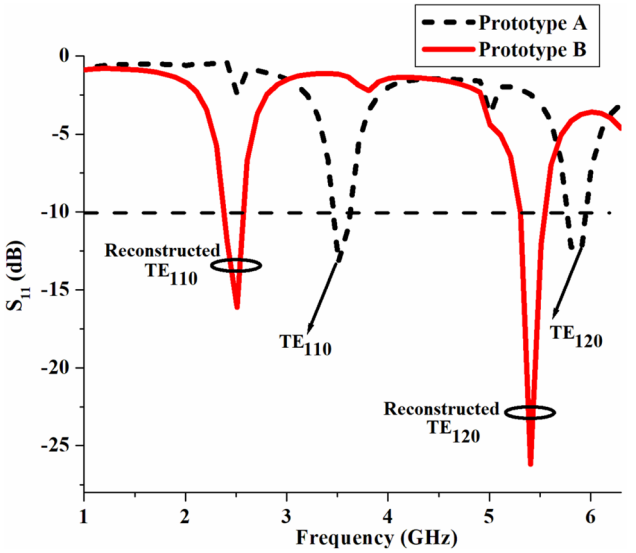

Fig. 3 S_{11}(dB) for prototype **A** and prototype **B**

4 Study of CSRR metamaterial

To confirm the resonance behavior, the complementary split ring resonator (CSRR) band nature is explained in this segment. The waveguide theory is utilized to perceive the scattering parameters for computing transmission (S_{21}) and reflection (S_{11}) coefficients of CSRR (Samson Daniel et al. 2018a). The S_{11}(dB) influences pass band nature owing to band pass filter for creating resonance characteristics and S_{21}(dB) influences stop band nature owing to band stop filter. Figure 6a describes the stop band (S_{21}) and pass band (S_{11}) nature of the CSRR metamaterial unit cell. It is understood that CSRR has two pass bands (S_{11}) at 2.5 GHz and 5.4 GHz. Here, 2.5 GHz supports the lower hybrid mode TE_{110}. Thus, it designates to be first order pass band f_0. Also, the hybrid mode TE_{120} (at 5.4 GHz) is attained at second order pass band $\approx 2f_0$, as detailed in Murugeshwari et al. 2019. These pass bands are beneficial for constructing dual operating bands in the proposed antenna design.

An effective permittivity (ε) of the CSRR is represented in Fig. 6b. It shows that the permittivity (ε) becomes negative at 2.5 GHz owing to first order pass band f_0 and at 5.4 GHz owing to second order pass band $\approx 2f_0$. Thus, the CSRR with optimized values have induced operating frequencies of 2.5 GHz and 5.4 GHz for designing dual band antenna.

Table 2 Examination of the designed antenna with previouslyreported work

References	Year	Patch detail	Antenna size L × W(mm^2)	Resonance Frequency (GHz)	Impedance Bandwidth (MHz)
Mukherjee and Biswas 2016)	2016	SIW cavity backed antenna loaded bow-tie slot	37 × 28.7	8.13 and 10.4	600 MHz (7.98–8.57 GHz) 888 MHz (9.72–10.6 GHz)
Mukherjee and Biswas 2017)	2017	SIW cavity backed antenna loaded dumbbell shaped slot	24 × 39	7.2, 9.36, and 14.30	60 MHz 250 MHz 250 MHz
Kumar et al. 2018)	2018	Self-diplexing antenna using SIW technique	32.5 × 32.5	6.44 and 7.09	160 MHz 200 MHz
Mukherjee and Biswas 2018)	2018	SIW technique with rectangular slot	78 × 22	9.6	670 MHz
Chaturvedi et al. 2019)	2019	Circular and rectangular SIW cavities loaded with circular slots	48 × 52	5.2 and 5.8	310 MHz (5.04–5.35 GHz) 190 MHz (5.73–5.92 GHz)
Nigam et al. 2020)	2020	SIW self-triplexing slot antenna	30.5 × 36.5	11.01, 12.15 and 13.1	Not Reported
Chaturvedi 2020)	2020	SIW antenna loaded slots with two metallic vias	42 × 24	5.7 and 5.85	340 MHz (5.57–5.91 GHz)
Priya et al. 2020)	2020	Self-Deplexing SIW Cavity-Backed Slot Antenna	32 × 34	11.2, 12.3 and 11.72	Not Reported
Designed antenna		SIW cavity backed antenna loaded with CSRR	30 × 30	2.5 and 5.4	100 MHz (2.45–2.55 GHz) 130 MHz (5.33–5.46 GHz)

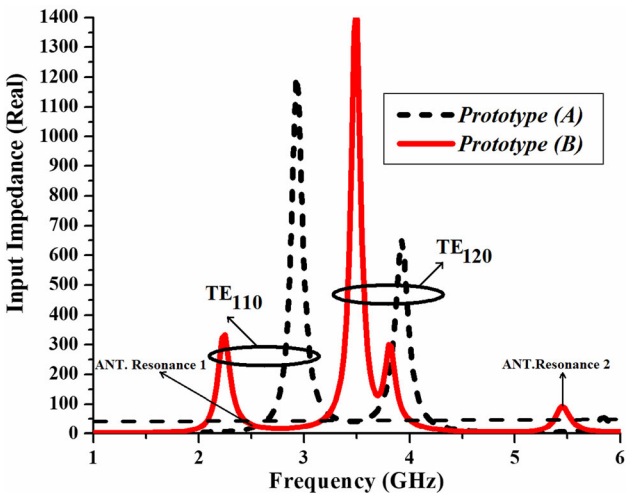

Fig. 4 Real part input impedance of the SIW cavity

5 Equivalent circuit investigation of CSRR

The resonance frequencies of complementary split ring resonator (CSRR) have been verified by an equivalent circuit (Mukherjee and Biswas 2017), as depicted in Fig. 7. The capacitance of the CSRR (C_{CSRR}) is influenced by slit surrounded by a slot and the inductance of the CSRR (L_{CSRR}) is influenced by slot surrounded by a slit. After introducing CSRR metamaterial, the reconstructed modes TE_{110} (at 2.5 GHz) and TE_{120} (at 5.4 GHz) are produced with better return loss characteristics. These resonance frequencies have been evaluated by Samson Daniel 2020

$$f_{CSRR} = \frac{1}{2\pi\sqrt{L_L C_L}} \tag{2}$$

where

$$C_{CSRR} = \frac{N-1}{2}[2L - (2N-1)(W+S)]C_0$$

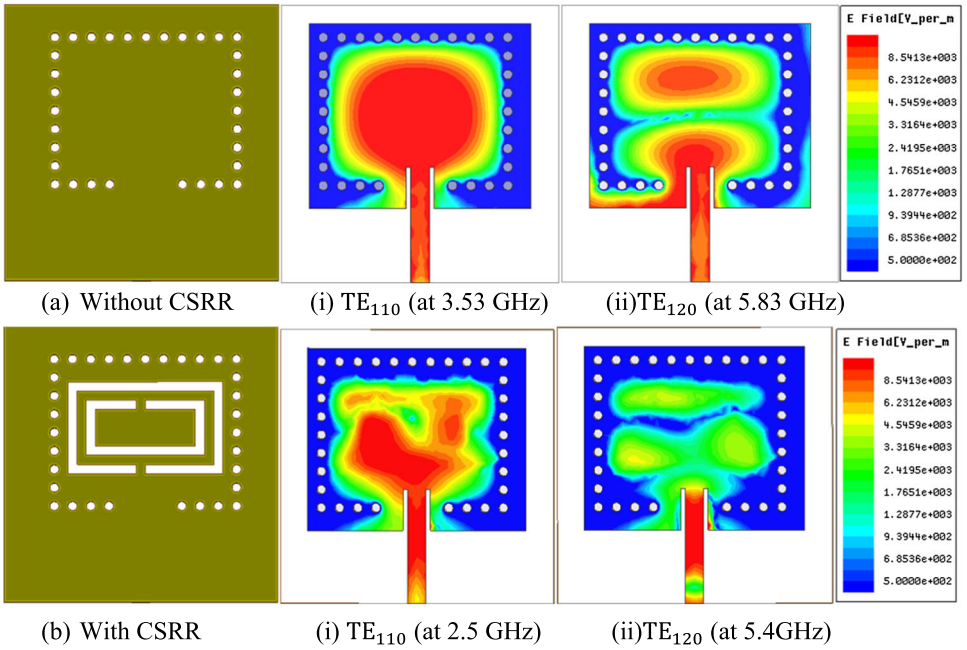

Fig. 5 Electric field distribution at the top view of substrate **a** without CSRR and **b** with CSRR

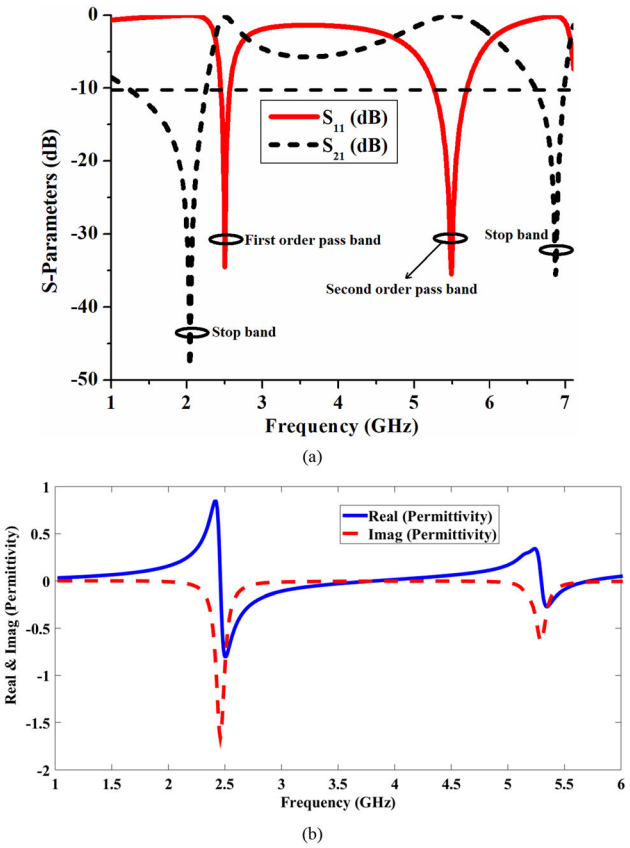

Fig. 6 **a** Scattering parameters of CSRR, **b** Permittivity of CSRR

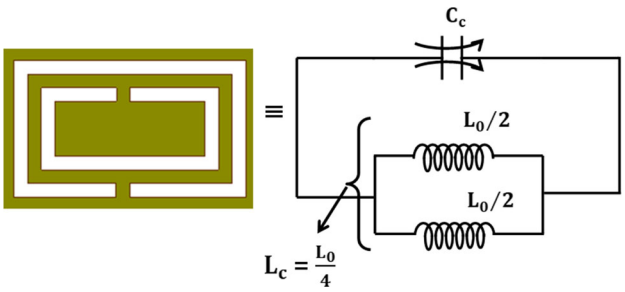

Fig. 7 Equivalent circuit topology

$$C_0 = \varepsilon_0 \frac{K\left(\sqrt{1-K^2}\right)}{K(k)} \quad \text{and} \quad k = \frac{S/2}{W + S/2}$$

$$L_{CSRR} = 4\mu_0 [L - (N-1)(S+W)] \left[\ln\left(\frac{0.98}{\rho}\right) + 1.84\rho\right]$$

$$\rho = \frac{(N-1)(W+S)}{1-(N-1)(W+S)}$$

Here, L is the average length of the CSRR ring, N = 2 number of rings, S = 1 mm spacing between two rings, W = 1 mm width of the ring and K(k) first order elliptical integral. These formulas are estimated by MATLAB program to determine CSRR resonance owing to inductance and capacitance values.

For outer ring CSRR, Average Length (L) = $\frac{l_1+W_1}{2}$ = 12.5 mm.

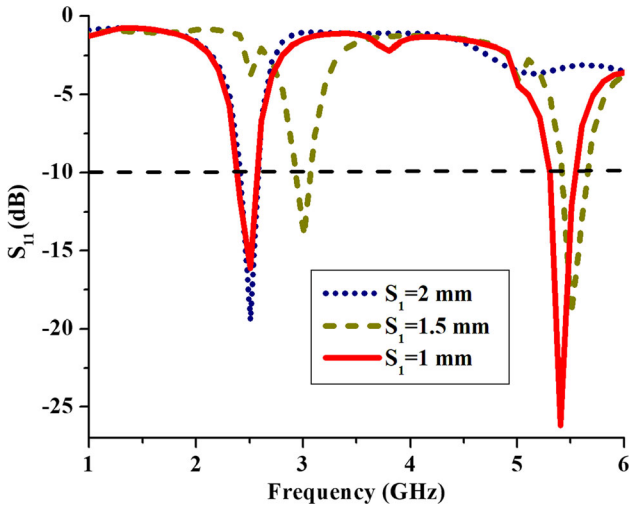

Fig. 8 Effect of CSRR slit (S_1) on S_{11}(dB)

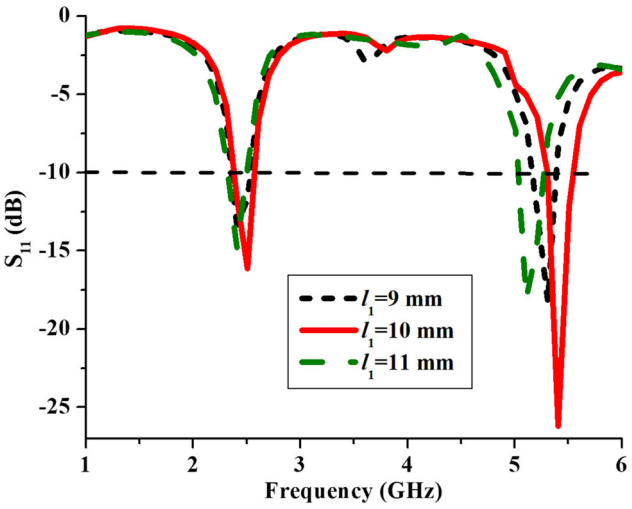

Fig. 10 Effect of CSRR length (l_1) on S_{11}(dB)

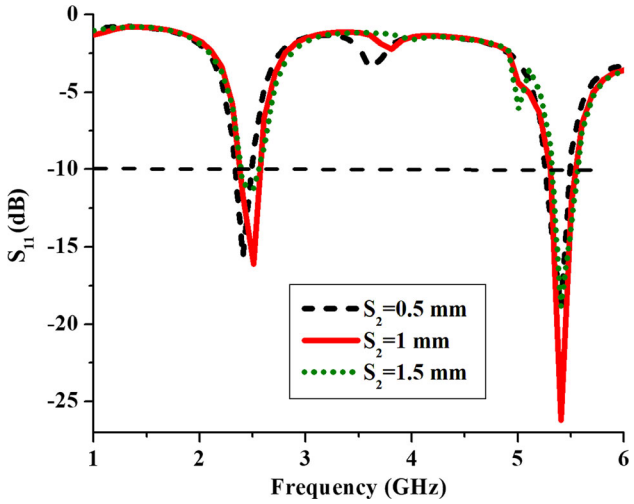

Fig. 9 Effect of CSRR width (S_2) on S_{11}(dB)

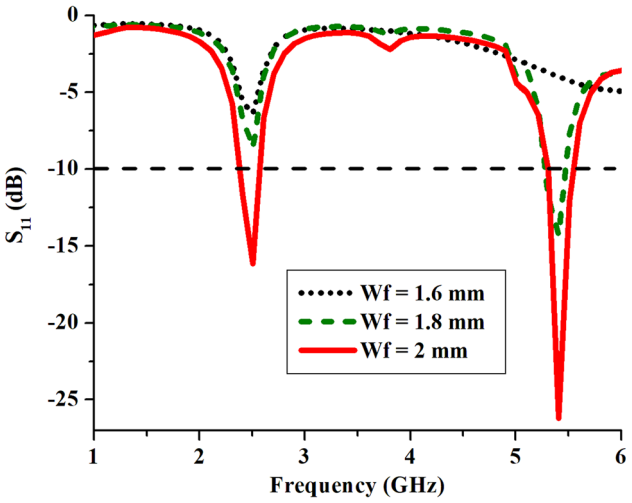

Fig. 11 Effect of feed width (W_f) on S_{11}(dB)

Hence, $C_{CSRR} = 7.5476 \times 10^{-14}$ (Farad) and L_{CSRR}= 5.3128 $\times 10^{-08}$ (Henry). So, the outer ring CSRR resonance frequencyis $f_{CSRR} = \frac{1}{2\pi\sqrt{L_{CSRR}C_{CSRR}}} = 2.51$GHz

For inner ring CSRR, Average Length (L) = $\frac{l_2+W_2}{2}$ = 8.5 mm.

Hence, C_{CSRR} = 3.2803 $\times 10^{-14}$ (Farad) and L_{CSRR}= 2.6173 $\times$ 10^{-08} (Henry). So, the inner ring CSRR resonance frequencyis $f_{CSRR} = \frac{1}{2\pi\sqrt{L_{CSRR}C_{CSRR}}} = 5.43$ GHz.

From this equivalent circuit topology, it predicts that CSRR yields resonance at 2.51 GHz and 5.43 GHz, which is recognized with simulated resonance at 2.5 GHz and 5.4 GHz.

6 Parametric study

The structural parameters of the antenna are minimized by evaluating S_{11}(dB) behavior of the CSRR slit (S_1), the width of the CSRR (S_2), length of the CSRR (l_1) and feed width (W_f). Figures 8 and 9 represents the variation of S_{11}(dB) on various dimensions of S_1 and S_2, respectively. Basically S_1(metal strip between the slots) governs the shunt inductance and S_2(slot between the metal strip) governs the series capacitance in the CSRR metamaterial. It can be revealed that both S_1 and S_2 contributes power to be distributed into the load for the first and second band

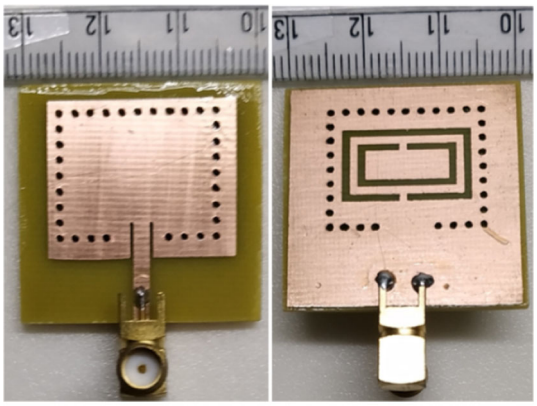

(a) (b)

Fig. 12 Picture of the fabricated antenna **a** Top view **b** Bottom view

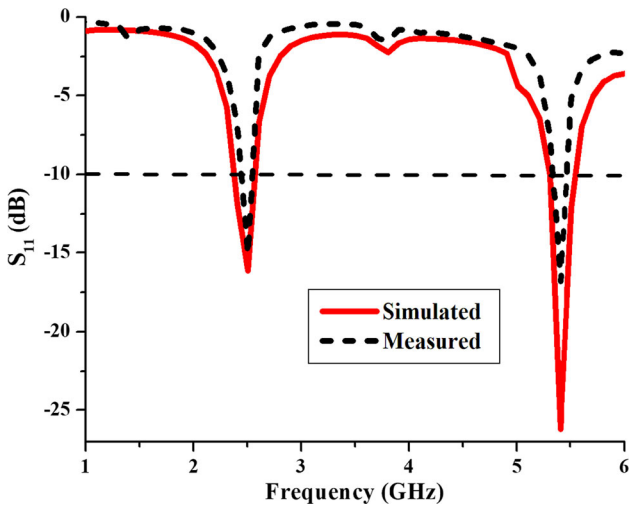

Fig. 13 S_{11}(dB) response of the proposed antenna

because of the connection between the CSRR on the ground plane and SIW cavity resonator.

Figure 10 describes the S_{11}(dB) by changing the length of the CSRR (l_1). It is inferred that this parameter plays an eminent impact for impedance matching of the second band. The higher order mode can be adjusted by series parameters instead of shunt parameters. However, this shunt parameter is capable of tuning lower resonance frequency. The width (W_f) of the microstrip feed line performs prominent role to drive the radiating modes and impedance characteristics. The feed width is increased from 1.6 mm to 2 mm and the conforming S_{11}(dB) characteristics are shown in Fig. 11. It is understood that by increasing the width of the microstrip feed, the dual band radiation with better impedance matching is obtained. Hence, the maximum possible value W_f = 2 mm is designated to resonance at 2.5 GHz and 5.4 GHz.

7 Measurement results

The proposed antenna is fabricated with the help of MITS PCB prototyping machine, which involves the process of creating photo film, printing layers, aligning the layers, drilling the holes, applying solder mask and silkscreen, final cutting. The major dimension of the fabricated prototype has high quality, reliability and extraordinary precision compared with designed antenna by using the Ansys HFSS electromagnetic tool. The picture of the fabricated antenna is shown in Fig. 12. Anritsu Vector Network Analyzer MS46122B has been used to measure the S_{11} (dB) of the fabricated antenna. An experimental and simulated S_{11}(dB) response of the designed antenna is explained in Fig. 13. Experimental data exhibits an –10 dB impedance bandwidth of 100 MHz (2.45–2.55 GHz) and 130 MHz (5.33–5.46 GHz) with 4% (f_c = 2.5 GHz) and 2.4% (f_c = 5.4 GHz) fractional bandwidths respectively. Figure 14 shows the normalized field pattern over the dual band radiation. The unidirectional and broadside radiation is obtained in E-plane (YZ plane) and H-plane (XZ plane) due to the SIW structural configuration. Experimental cross-polarization components are –23 dB and –15 dB in the E-plane and –24 dB and 19 dB in the H-plane at 2.5 GHz and 5.4 GHz, respectively.

The peak gain values of the antenna have been computed using gain transfer procedure (Samson Daniel et al. 2018b) and plotted in Fig. 15. In this method, the experimental peak gains are obtained by measuring the ratio of peak power of the fabricated antenna under test with the standard gain horn antenna. It provides an experimental peak gain of 3.43 dBi at 2.5 GHz and 5.31 dBi at 5.4 GHz. Basically metamaterial elements induce a negative or low

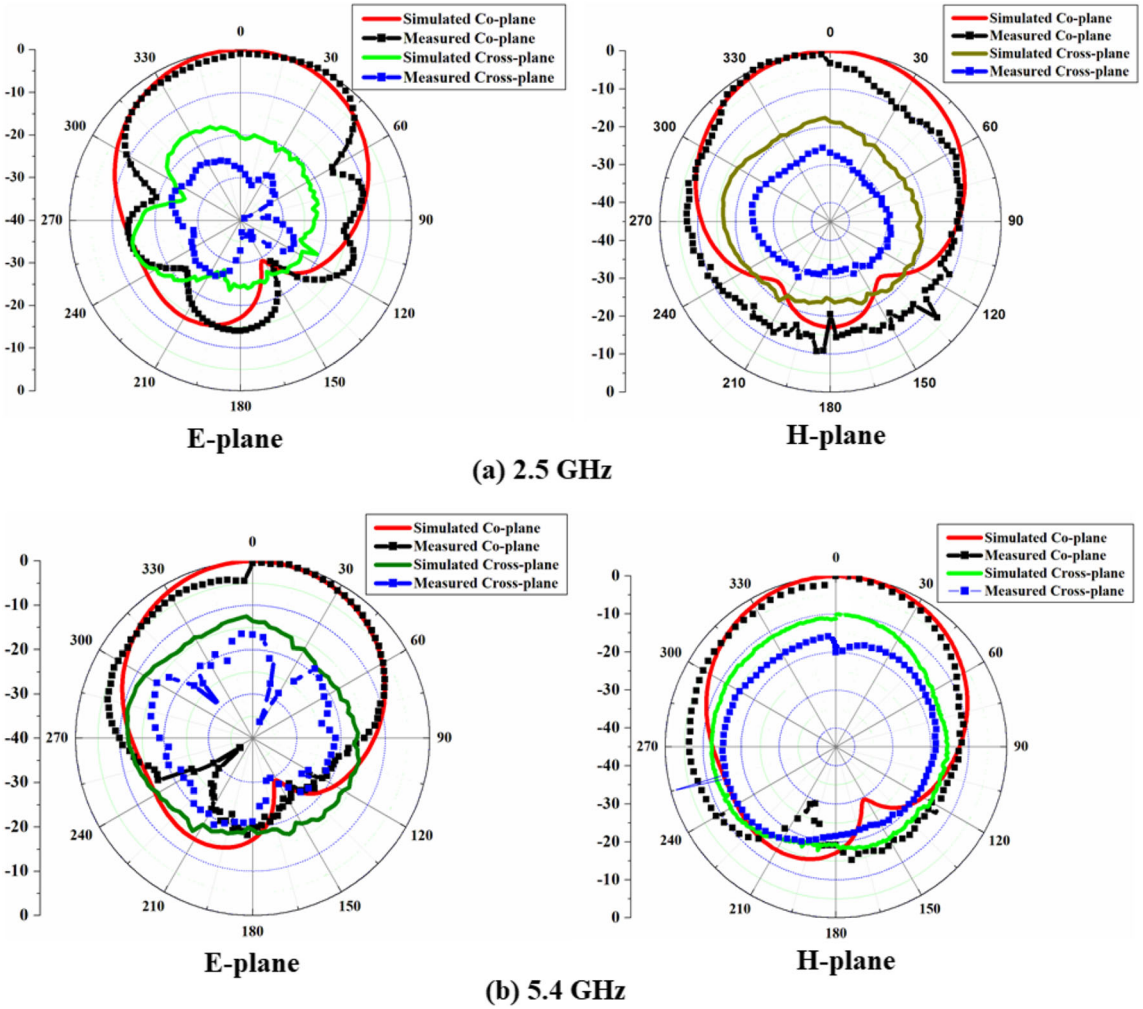

Fig. 14 E-plane and H-plane radiation patterns **a** 2.5 GHz **b** 5.4 GHz

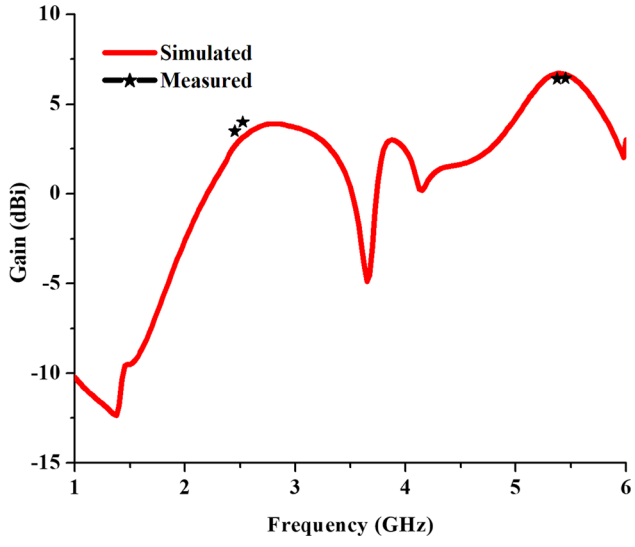

Fig. 15 Proposed antenna gain plot

gain value in the lower resonance frequency (Samson Daniel 2020) due to antenna compactness. Thus, the high level of antenna miniaturization affects radiation characteristics which leads to reduce the gain.

8 Conclusion

A low-profile complementary split ring resonator loaded SIW cavity backed antenna is designed using mode theory mechanism for dual band radiation. It exposes that CSRR is essential in addition to the rectangular SIW cavity resonator, to obtain lower hybrid modes TE_{110} and TE_{120} for reducing the size of the antenna. The performance of the proposed configuration has been elucidated by parametric examination. An electrical size of the designed antenna is $0.25\ \lambda_0 \times 0.25\ \lambda_0 \times 0.0133\ \lambda_0$. The fabricated antenna has low-profile geometry and its radiation characteristics are tested. The measured radiation pattern exhibits

unidirectional and lower cross polarization power levels for 2.5 GHz WiMAX and 5.4 GHz WLAN applications.

Data availability All data generated or analysed during this study are included in this published article (and its supplementary information files).

References

Cao M-S, Wang X-X, Zhang M, Shu J-C, Cao W-Q, Yang H-J, Fang X-Y, Yuan J (2019) Electromagnetic response and energy conversion for functions and devices in low-dimensional materials. Adv Func Mater 29(25):1807398

Cao M-S, Wang X-X, Zhang M, Cao W-Q, Fang X-Y, Yuan J (2020) Variable-temperature electron transport and dipole polarization turning flexible multifunctional microsensor beyond electrical and optical energy. Adv Mater 32(10):1907156

Chaturvedi D (2020) SIW cavity-backed 24 ° inclined-slots antenna for ISM band application. Int J RF Microw Comput Aided Eng 30(5):e22160

Chaturvedi D, Kumar A, Raghavan S (2019) A nested siw cavity-backing antenna for Wi-Fi/ISM band applications. IEEE Trans Antennas Propag 67(4):2775–2780

Gatti RV, Rossi R (2018) Hermetic Broadband 3-dB Power Divider/Combiner in Substrate-Integrated Waveguide (SIW) Technology. IEEE Trans Microwave Theory Techn 66(6):3048–3054

Gong L, Chan KY, Ramer R (2016) Substrate Integrated Waveguide H-Plane horn antenna with improved front-to-back ratio and reduced side lobe level. IEEE Antennas Wirel Propag Lett 15:1835–1838

Gong L, Chan KY, Ramer R (2017) Phase correction of the electric field for a dielectric loaded substrate integrated waveguide H-plane horn antenna. Microwave Opt TechnolLett 59(3):584–588

Kumar A, Chaturvedi D, Raghavan S (2018) Design of a self-diplexingantenna using SIW technique with high isolation. AEU Int J Electron C 94:386–391

Mukherjee S, Biswas A (2018) Design of planar high-gain antenna using SIW cavity hybrid mode. IEEE Trans Antennas Propagat 66(2):972–977

Mukherjee S, BiswasA A (2016) Design of dual band and dual-polarised dual band SIW cavity backed bow-tie slot antennas. IET Microw Antenn Propag 10(9):1002–1009

Mukherjee S, BiswasA A (2017) Computer aided equivalent circuit model of SIW cavity backed triple band slot antenna. Int J RF Microw Comput Aided Eng 27(2):e21060

Murugeshwari B, SamsonDaniel R, Raghavan S (2019) A compact dual band antenna based on metamaterial-inspired split ring structure andhexagonal complementary split-ring resonator for ISM/WiMAX/WLAN applications. Appl Phys A 125:628

Nigam P, Agarwal R, Muduki A, Sharma S, Pal A (2020) Substrate integrated waveguide based cavity-backed self-triplexing slot antenna for X-ku band applications. Int J RF Microw Comput Aided Eng 30(4):e22172

Priya S, Kumar K, Dwari S, Mandal MK (2020) Circularly polarized self-deplexing SIW cavity-backed slot antennas. IEEE Trans Antennas Propagat 68(3):2387–2392

Samson Daniel R (2020) Broadband μ-negative antenna using ELC unit cell. AEU Int J Electron C 118:153147

Samson Daniel R, Pandeeswari R, Raghavan S (2018a) A compact metamaterial loaded monopole antenna with offset-fed microstrip line for wireless applications. AEU Int J Electron C 83:88–94

Samson Daniel R, Pandeeswari R, Raghavan S (2018b) A miniaturized printed monopole antenna loaded with hexagonal complementary split ring resonators for multiband operations. Int J RF Microw Comput Aided Eng 28:e21401

Samson Daniel R, Pandeeswari R, Raghavan S (2018c) Dual-band monopole antenna loaded with ELC metamaterial resonator for WiMAX and WLAN applications. Appl Phys 124:570

Shi L-F, Sun C-Y, Chen S, Liu G-X, Shi Y-F (2018) Dual-band substrate integrated waveguide bandpass filter based on CSRRs and multimode resonator. Int J RF Microw Comput Aided Eng 28(9):e21412

Yun T, Lim S (2014) High-Q and miniaturized complementary split ring resonator-loaded substrate integrated waveguide microwave sensor for crack detection in metallic materials. Sens Actuators, A 214:25–30

Zhang M, Cao M-S, Shu J-C, Cao W-Q, Li L, Yuan J (2021) Electromagnetic absorber converting radiation for multifunction. Mater Sci Eng R Rep 145:100627